

# Analytic eigenvalue structure of the one-dimensional Dirac oscillator

Bo-Xing Cao and Fu-Lin Zhang\*

Department of Physics, School of Science, Tianjin University, Tianjin 300072, China

(Dated: December 21, 2024)

We study the analytic structure for eigenvalues of the one-dimensional Dirac oscillator, by analytically continuing its frequency on the complex plane. A twofold Riemann surface is found connecting the two states of a pair of particle and antiparticle. One can, at least in principle, accomplish the transition from a positive energy state to its antiparticle state, by moving the frequency continuously on the complex plane, without changing the Hamiltonian after transition. This result provides a visual explanation for the absence of a negative energy state with the quantum number  $n = 0$ .

Keywords:

## I. INTRODUCTION

Experimental studies of exceptional points in several systems [1–5] make the functions of a complex variable being no longer limited to an abstract tool in physics. On the other hand, very recently, the structure of the Riemann surface for quantum systems attracts theoretical research of Bender *et. al.* [6, 7]. Namely, in the system of two coupled harmonic oscillators, they show an eightfold Riemann surface structure of eigenvalues as functions of the complex coupling parameter, which collapses to a fourfold one in the case of the ground state. In the decoupling limit, these eigenvalues can be cast into sets of four eigenvalues, one corresponding to a conventional state, and the other three to unconventional states with negative energy. These unconventional states, which are nonnormalizable, can also be reached by analytically continuing the frequencies of isolated harmonic oscillators [8].

These progresses prompt us to consider the relativistic version of the harmonic oscillator, known as the Dirac oscillator [9, 10], whose eigenvalues are positive-negative in pairs. The Dirac oscillator is obtained from the free Dirac equation by the substitution  $\mathbf{p} \rightarrow \mathbf{p} - i\beta m\omega\mathbf{x}$ , where  $\omega$  is the frequency of the oscillator and  $\beta$  is a Dirac matrix. It exhibits abundant algebraic properties [11–15], and is used in various branches of physics, such as nuclear physics [16] and subnuclear physics [17]. Recently, there has been a growing interest in simulating the Dirac oscillator in other physical systems, such as quantum optics [18–21] and classical microwave setups [22, 23].

We focus on the Dirac oscillator in one spatial dimension, which also can be derived by linearizing the quadratic form  $E^2 = p^2 + m^2 + m\omega^2 x^2 - \beta m\omega$ , as Dirac's original approach to propose his equation [24]. Therefore, it naturally has the property of a square root, which is a key cause of the structure of Riemann surface in the non-relativistic harmonic systems [6–8]. It can be regarded as a coupled quantum system, which is the starting points of the study [6], as it maps exactly onto Jaynes-Cummings

model in quantum optics [21], composed by a harmonic oscillator and a spin. Furthermore, the experimental progresses in microwave setups, on simulating the Dirac oscillator [23] and observing exceptional points [1–3], make it possible to experimentally observe the Riemann surface studied in the present work.

We find a twofold Riemann surface structure for the eigenvalues, of the one-dimensional Dirac oscillator, as functions of the frequency parameter  $\omega$ . Such surface connects two conventional states of a particle with its antiparticle, which have the same quantum number  $n$ . By moving the system through a branch cut on the complex-frequency plane, one can move a positive energy state to its antiparticle state. From this angle of view, the disappearance of the branch point provides an interpretation for the absence of negative energy state with  $n = 0$ . Similar to the nonrelativistic harmonic oscillator, an unconventional spectrum arises in the analytic continuation. However, the conventional states and unconventional states locate on different Riemann surfaces, which is different from the harmonic oscillator.

In Sec.II, we review the analytic structure of one-dimensional harmonic oscillator. Based on these results, we study the Dirac oscillator in detail in Sec.III. Finally, a brief summary is given in Sec. IV.

## II. HARMONIC OSCILLATOR

The Hamiltonian of a nonrelativistic harmonic oscillator reads

$$H = \frac{1}{2m}p^2 + \frac{1}{2}m\omega^2 x^2. \quad (1)$$

In this work, we set the reduced Planck constant  $\hbar = 1$ . In the asymptotic region  $|x| \rightarrow +\infty$ ,  $m\omega^2 x^2 \gg E$ , the stationary Schrödinger equation reads

$$\phi'' = m^2\omega^2 x^2 \phi. \quad (2)$$

Its approximate solutions can be written as

$$\phi = e^{f(x)}, \quad (3)$$

---

\*Corresponding author: flzhang@tju.edu.cn

in which  $f(x) = \pm \frac{1}{2}m\omega x^2$  is derived from

$$[f'(x)]^2 = m^2\omega^2 x^2. \quad (4)$$

Making the substitutions  $\xi = \sqrt{m\omega}x$ ,  $k = 2E/\omega$  and  $\phi(\xi) = h(\xi)e^{\mp\xi^2/2}$ , one obtains

$$\frac{d^2h}{d\xi^2} \mp 2\xi \frac{dh}{d\xi} + (k \mp 1)h = 0. \quad (5)$$

It is the defining differential equation for the Hermite polynomials if  $k = \pm(2n+1)$  and  $n = 0, 1, 2, \dots$ , which can be represented as

$$h_{\pm n}(\xi) = (\pm 1)^n e^{\mp\xi^2} \frac{\partial^n}{\partial \xi^n} e^{\pm\xi^2}. \quad (6)$$

The plus sign corresponds to the conventional Hermite polynomials,  $H_n(\xi) = h_{+n}(\xi)$ , and the consequently conventional eigenfunctions of harmonic oscillator. We denote the ones with minus sign as  $h_{-n}(\xi)$ , which leads to nonnormalizable unconventional eigenfunctions [6]. Then, the eigenvalues and corresponding eigenfunctions are

$$E_n^\pm = \pm(n + \frac{1}{2})\omega, \quad \phi_n^\pm(\xi) = h_{\pm n}(\xi)e^{\mp\frac{1}{2}\xi^2}. \quad (7)$$

Obviously, the  $\pm$  signs in the above results come from the square root of Eq. (4). Consequently, the eigenvalues with the same quantum number  $n$  are merely different branches of a multivalued function of complex  $\omega$ , which can be written as

$$E_n(\omega) = \pm(n + \frac{1}{2})\sqrt{\omega^2} = (n + \frac{1}{2})e^{\frac{1}{2}\text{Ln}(\omega^2)}. \quad (8)$$

With the aid of the logarithmic function in above expression, one can easily notice the connection structure of the function.

In Fig. 1, we show the real part of the Riemann surface for  $n = 0$ . The function is unchanged under  $\omega \rightarrow -\omega$ , which can be traced back to the symmetry of the Hamiltonian (1). However, the eigenvalues change sign, as the argument of  $\omega$  runs continuously from 0 to  $\pi$ . There are two coalescing branch points at  $\omega = 0$ , and the two associated branch cuts can be chosen along the imaginary  $\omega$  axis. Each additional  $\pi$  on the argument of  $\omega$  moves the system from one branch to another, and changes the sign of eigenvalues though the Hamiltonian remains unchanged. Simultaneously, the variable  $\xi$  is changed into  $i\xi$ , which leads to

$$\phi_n^+(\xi) \rightarrow \phi_n^+(i\xi) = -i^n \phi_n^-(\xi). \quad (9)$$

That is, by such analytic continuation, we reach an unconventional state, starting from a conventional one. A similar process can move the system from a conventional state to an unconventional one.

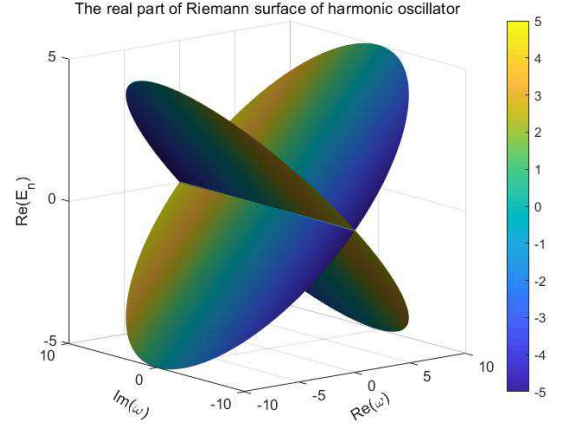


FIG. 1: (Color online) The real part of the Riemann surface for one-dimensional harmonic oscillator with the quantum number  $n = 0$ . The imaginary part is shown by color.

### III. DIRAC OSCILLATOR

#### A. Spectra

The Dirac oscillator has become the paradigm for the construction of covariant quantum models with some well determined nonrelativistic limit [23], and its properties and possible applications have been studied extensively. To be corresponding to the above section, we study the one-dimensional version of the Dirac oscillator in this part, whose Hamiltonian is given by

$$\mathcal{H} = \alpha(p - i\beta m\omega x) + \beta m, \quad (10)$$

with the light velocity  $c = 1$ . The Dirac matrices are conveniently defined in terms of the Pauli matrices

$$\alpha = \sigma_y, \quad \beta = \sigma_z. \quad (11)$$

To understander its spectra, we square the Hamiltonian (10) and obtain

$$\mathcal{H}^2 = m^2 + p^2 + m^2\omega^2 x^2 - \beta m\omega. \quad (12)$$

When  $\mathcal{H} \rightarrow m$ ,

$$\begin{aligned} \mathcal{H} - m &= \frac{\mathcal{H}^2 - m^2}{\mathcal{H} + m} \\ &\rightarrow \frac{\mathcal{H}^2 - m^2}{2m} = \frac{p^2}{2m} + \frac{1}{2}m\omega^2 x^2 - \frac{1}{2}\beta\omega. \end{aligned} \quad (13)$$

That is, in the nonrelativistic limit, the Dirac oscillator becomes a decoupled system composed of a harmonic oscillator and a spin.

The relations in (12) and (13) make it direct to derive the eigenvalues and eigenfunctions of  $\mathcal{H}^2$  based on the results of the harmonic oscillator. Corresponding to each

eigenvalue in (7), one can obtain the one of  $\mathcal{H}^2$  as

$$\mathcal{E}^2 = m^2 \pm 2nm\omega. \quad (14)$$

and the two-component eigenfunctions

$$\psi_n^+ = \begin{pmatrix} a_n^+ \phi_n^+(\xi) \\ b_n^+ \phi_{n-1}^+(\xi) \end{pmatrix}, \quad \psi_n^- = \begin{pmatrix} a_n^- \phi_{n-1}^-(\xi) \\ b_n^- \phi_n^-(\xi) \end{pmatrix}, \quad (15)$$

where we denote  $\phi_{-1}^\pm(\xi) = \phi_0^\mp(\xi)$  and  $\xi = \sqrt{m\omega}x$ . And,  $a_n^\pm$  and  $b_n^\pm$  are free parameters, which is due to the double degenerate caused by the resonance between the spin and harmonic oscillator in (13). The states  $\psi_0^+$  and  $\psi_0^-$  represent the same degenerate subspace.

Diagonalizing the Hamiltonian in the degenerate subspaces of  $\mathcal{H}^2$ , one can find the eigenfunctions of  $\mathcal{H}$

$$\Psi_{\pm n}^+ = \begin{pmatrix} (m \pm \sqrt{m^2 + 2nm\omega})\phi_n^+(\xi) \\ 2n\sqrt{m\omega}\phi_{n-1}^+(\xi) \end{pmatrix}, \quad (16)$$

$$\Psi_{\pm n}^- = \begin{pmatrix} 2n\sqrt{m\omega}\phi_{n-1}^-(\xi) \\ (m \mp \sqrt{m^2 - 2nm\omega})\phi_n^-(\xi) \end{pmatrix}, \quad (17)$$

corresponding to the eigenvalues

$$\mathcal{E}_{\pm n}^\pm = \pm \sqrt{m^2 \pm 2nm\omega}, \quad (18)$$

where the subscripts indicate the signs before the square roots, and the superscripts indicate the ones in the square roots. When  $n = 0$ ,  $\Psi_{-0}^+$  and  $\Psi_{+0}^-$  vanish, and the eigenenergies  $\mathcal{E}^\pm = \pm m$  corresponds to the states  $\Psi_{+0}^+$  and  $\Psi_{-0}^-$  respectively. And the lower/upper component in  $\Psi_{+0}^+/\Psi_{-0}^-$  is zero. These results indicate that, the conventional and unconventional states appear separately in  $\Psi_{\pm n}^+$  and  $\Psi_{\pm n}^-$ . Hence, we refer to  $\Psi_{\pm n}^-$  as the unconventional eigenfunctions of the Dirac oscillator, as  $\Psi_{\pm n}^+$  are the conventional ones [25].

## B. Analytic structure

We now turn to the analytic structure of the Dirac oscillator. The eigenvalue (18) with a fixed quantum number  $n \neq 0$  is actually a nested square-root function, as the inner  $\pm$  signs are from the square root to derive the eigenfunctions of the Harmonica oscillator. Hence one can rewrite the eigenvalue as

$$\mathcal{E}_n(\omega) = \pm \sqrt{m^2 \pm 2nm\sqrt{\omega^2}}. \quad (19)$$

It has six square-root branch points, four occurring at  $\omega = 0$  and two at  $\omega = \pm m/(2n)$ . The associated branch cuts at  $\omega = 0$  are choosed along the imaginary  $\omega$  axis, and the ones at  $\omega = \pm m/(2n)$  along the real  $\omega$  axis. They connect four sheets of the Riemann surface pairwise to

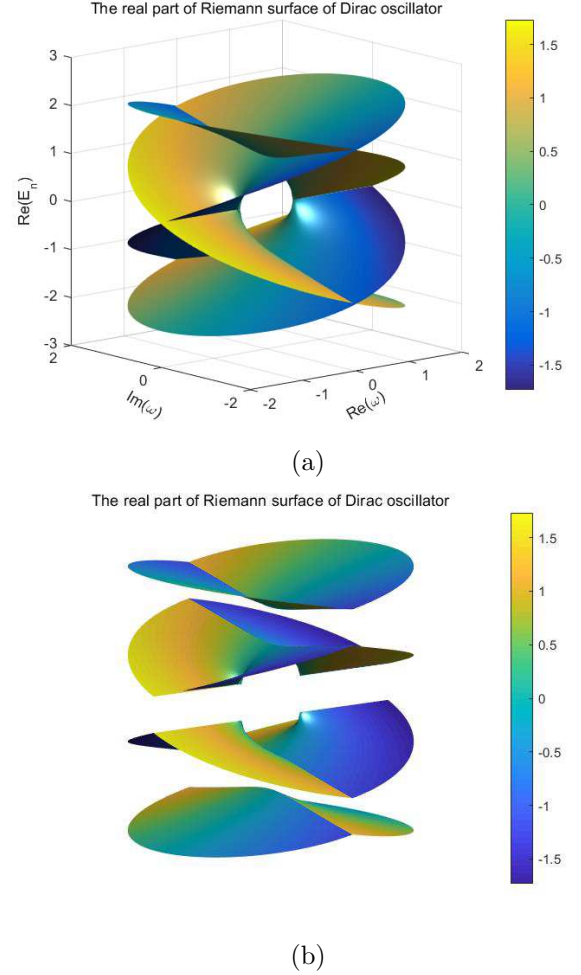


FIG. 2: (Color online) (a) The real part of Riemann surface of  $\mathcal{E}_n(\omega)$  with  $m = 1$  and  $n = 1$ . Shapes of the four sheets of the function are shown in (b). The amount of imaginary part is shown by color.

one another.

A visualization of this surface and its four sheets is shown in Fig. 2. Let us take a brief look at the function. We start from a positive real  $\omega = |\omega| > m/(2n)$  and  $\mathcal{E}_n(\omega) = \sqrt{m^2 + 2nm\sqrt{\omega^2}}$ , which locates on the top sheet. Increasing the phase  $\theta$  of  $\omega = e^{i\theta}|\omega|$ , one can enter the second sheet after pass through the positive-imaginary axis. Next, running  $\theta$  to the region of  $(\pi, 3\pi/2)$ , one get the third sheet. Follow that, when  $\omega$  reaches the fourth quadrant,  $\mathcal{E}_n(\omega)$  enters its fourth sheet, where  $\mathcal{E}_n(\omega) = -\sqrt{m^2 + 2nm\sqrt{\omega^2}}$  when  $\theta = 2\pi$ . If the phase  $\theta$  continues to increase, the function reenters the third, second, and first sheets in turn. When  $\theta = 4\pi$ ,  $\mathcal{E}_n(\omega)$  gets back to the initial point.

An obvious feature of the above route is that, it goes through the first and fourth sheets when  $\text{Re}(\omega) > 0$ , and through the second and third ones when  $\text{Im}(\omega) > 0$ . The four regions actually compose the Riemann surface

of

$$\mathcal{E}_n^+(\omega) = \pm\sqrt{m^2 + 2nm\omega}, \quad (20)$$

which is a half of the function  $\mathcal{E}_n(\omega)$ . Starting from a negative real  $\omega = -|\omega|$  on the top sheet, one gets a route going through the other half,

$$\mathcal{E}_n^-(\omega) = \pm\sqrt{m^2 - 2nm\omega}. \quad (21)$$

Although, a similar feature can be found in the Harmonic oscillator, the difference is that the symmetry of  $\omega \rightarrow -\omega$  is broken in the Dirac oscillator, which can be easily noticed by the linear terms in (12) and (13). Starting from one of the conventional states in (16), it is impossible to reach an unconventional one by smoothly varying the frequency  $\omega$ .

Based on the above considerations, from a viewpoint of succinctness,  $\mathcal{E}_n^+(\omega)$  and  $\mathcal{E}_n^-(\omega)$  should be regarded as two distinct functions, which connect the conventional states and the unconventional states respectively. To show the connection structures, we take the conventional states for example. The results of the unconventional states can be easily obtained by simultaneously changing the two  $\pm$  signs in (18) and flipping the spin.

The function  $\mathcal{E}_n^+(\omega)$  has one square-root branch point at  $\omega = -m/(2n)$  when  $n \neq 0$ , and the associated branch cut can be chosen along the negative-real axis. We show the Riemann surface in Fig. 3. Let the Dirac oscillator start from a positive energy state  $\Psi_{+n}^+$  with  $\mathcal{E}_n^+(\omega) = +\sqrt{m^2 + 2nm\omega}$ , we run the argument  $\theta$  of  $\omega = e^{i\theta}|\omega|$  from 0 to  $2\pi$ . When  $|\omega| < m/(2n)$ , the system gets back to the initial state  $\Psi_{+n}^+$ . When  $|\omega| > m/(2n)$ , the system passes through the branch cut, and reaches its antiparticle state  $\Psi_{-n}^+$  with a negative energy  $\mathcal{E}_n^+(\omega) = -\sqrt{m^2 + 2nm\omega}$ .

In the transition between a state to its antiparticle state, the eigenvalue becomes complex when  $\theta = \pi$  reflecting that the system is in a region of broken PT symmetry, which is also noticed in the system of two coupled harmonic oscillators [7]. The amount of  $|\omega|$  to break the PT symmetry increases with the quantum number  $n$  decreases. When  $n = 0$ , it can be considered to become  $+\infty$ . This result provides a visual explanation for the absence of  $\Psi_{-0}^+$ .

#### IV. SUMMARY

We study the analytic structure of eigenvalues of the Dirac oscillator in one spatial dimension. There exist four eigenfunctions corresponding to an oscillator quantum number  $n$ , two of which are conventional states for a pair of particle and antiparticle, and the other two are unconventional. The two conventional states are connected by a twofold Riemann surface, for the eigenvalues as a function of frequency on the complex plane. So are the two unconventional states. The system can be

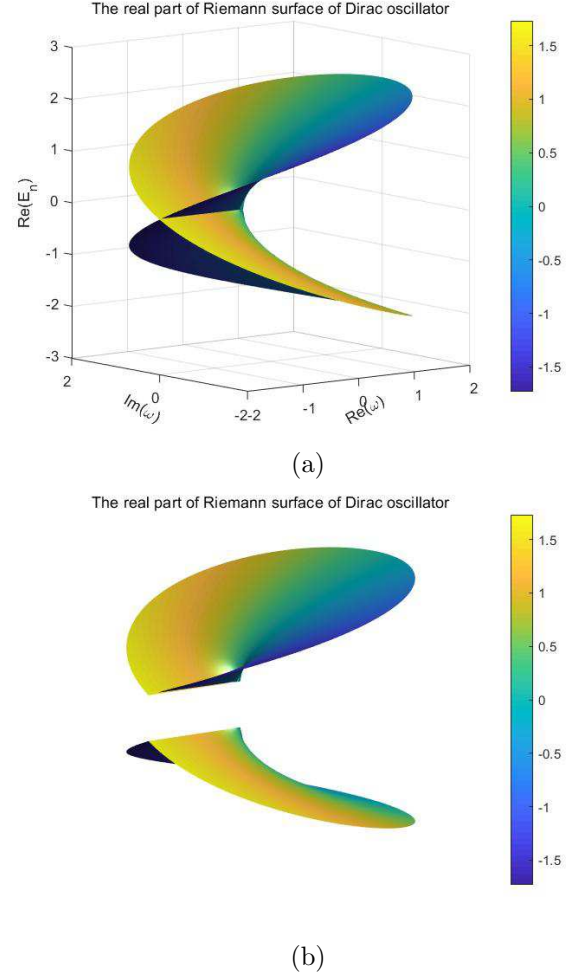


FIG. 3: (Color online) (a) The real part of Riemann surface of  $\mathcal{E}_n^+(\omega)$  with  $m = 1$  and  $n = 1$ . Shapes of the two sheets of the function are shown in (b). The amount of imaginary part is shown by color.

transitioned smoothly among the states by an analytic continuation in the frequency constant. Based on these results, the absence of a negative energy state with  $n = 0$  can be intuitively explained by the disappearance of the branch point.

Further researches on this topic in several directions would be interesting. First, we look forward to an experimental verification of the analytic continuation studied in this work. Also, it is fascinating to consider the Berry phases [26] acquired by the system when it moves on the Riemann surfaces. Whether more elaborate structures arise from the Riemann surfaces in the two- or three-dimensional Dirac oscillators is also a natural question. Finally, could we give a physical meaning of the unconventional states? Or more specifically, whether the negative energy of an unconventional state in nonrelativistic harmonic oscillators [6–8] is a positive one actually, as the negative energy in the Dirac equation?

## Acknowledgments

This work is supported by NSF of China (Grant No.11675119, No.11575125, No.11105097). We thank

Wen-Ya Song, Wu-Sheng Dai and Yun-Peng Liu for their discussions.

- 
- [1] C. Dembowski, H.-D. Gräf, H. L. Heine, W. D. Heiss, H. Rehfeld, and A. Richter, Phys. Rev. Lett. **86**, 787 (2001).
  - [2] B. Dietz, H. L. Harney, O. N. Kirillov, M. Miski-Oglu, A. Richter, and F. Schäfer, Phys. Rev. Lett. **106**, 150403 (2011).
  - [3] J. Doppler, A. A. Mailybaev, J. Böhm, U. Kuhl, A. Girschik, F. Libisch, T. J. Milburn, P. Rabl, N. Moiseyev, and S. Rotter, Nature **537**, 76 (2016).
  - [4] W. Chen, S. K. Özdemir, G. Zhao, J. Wiersig, and L. Yang, Nature **548**, 192 (2017).
  - [5] H. Xu, D. Mason, L. Jiany, and J. G. E. Harris, Nature **537**, 80 (2016).
  - [6] C. M. Bender, A. Felski, N. Hassanpour, S. P. Klevansky, and A. Beygi, Phys. Scr. **92**, 015201 (2017).
  - [7] A. Felski and S. P. Klevansky, Phys. Rev. A **98**, 012127 (2018).
  - [8] C. M. Bender and A. Turbiner, Phys. Lett. A **64**, 442 (1993).
  - [9] M. Moshinsky and A. Szczepaniak, J. Phys. A: Math. Gen. **98**, 817 (1989).
  - [10] E. Sadurní, AIP Conf. Proc. **1334**, 249 (2010).
  - [11] O. L. de Lange, J. Phys. A: Math. Gen. **24**, 667 (1991).
  - [12] J. Benitez, Phys. Rev. Lett. **64**, 1643 (1990).
  - [13] C. Quesne and M. Moshinsky, J. Phys. A: Math. Gen. **23**, 2263 (1990).
  - [14] R. Lisboa, M. Malheiro, A. S. de Castro, P. Alberto, and M. Fiolhais, Phys. Rev. C **69**, 024319 (2004).
  - [15] F.-L. Zhang, B. Fu, and J.-L. Chen, Phys. Rev. A **80**, 054102 (2009).
  - [16] J. Grineviciute and D. Halderson, Phys. Rev. C **85**, 054617 (2012).
  - [17] E. Romera, Phys. Rev. A **84**, 052102 (2011).
  - [18] A. Bermudez, M. A. Martin-Delgado, and E. Solano, Phys. Rev. A **76**, 041801 (2007).
  - [19] A. Bermudez, M. A. Martin-Delgado, and E. Solano, Phys. Rev. Lett. **99**, 123602 (2007).
  - [20] L. Lamata, J. León, T. Schätz, and E. Solano, Phys. Rev. Lett. **98**, 253005 (2007).
  - [21] J. M. Torres, E. Sadurn, and T. H. Seligman, AIP Conf. Proc. **1323**, 301 (2010).
  - [22] E. Sadurní, T. H. Seligman, and F. Mortessagne, New J. Phys. **12**, 053014 (2010).
  - [23] J. A. Franco-Villafañe, E. Sadurní, S. Barkhofen, U. Kuhl, F. Mortessagne, and T. H. Seligman, Phys. Rev. Lett. **111**, 170405 (2013).
  - [24] P. A. M. Dirac, *The principles of Quantum Mechanics* (Oxford University Press 1930, 1965).
  - [25] R. Szmytkowski and M. Gruchowski, J. Phys. A: Math. Gen. **34**, 4991 (2001).
  - [26] M. V. Berry, Proc. R. Soc. London, Ser. A **392**, 45 (1984).